European Journal of Pharmacology 666 (2011) 242–250

Contents lists available at ScienceDirect

European Journal of Pharmacology

journal homepage: www.elsevier.com/locate/ejphar

Immunopharmacology and Inflammation

Anti-oxidative and TNF-α suppressive activities of puerarin derivative (4AC) in RAW264.7 cells and collagen-induced arthritic rats

Cheng Xiao [a,1], Jian Li [b,c,1], Xinxin Dong [c], Xiaojuan He [c], Xuyan Niu [c], Cha Liu [d], Guoyue Zhong [e], Rudolf Bauer [f], Dajian Yang [d,e,*], Aiping Lu [c,**]

[a] China–Japan Friendship Hospital, Beijing, PR China
[b] Beijing University of Chinese Medicine, Beijing, PR China
[c] Institute of Basic Research in Clinical Medicine, China Academy of Chinese Medical Science, Beijing, PR China
[d] State Key Laboratory Incubation Base of Chinese Medicine and Molecular Pharmacology, Shenzhen, PR China
[e] Chongqing Academy of Chinese Materia Medica, Chongqing, PR China
[f] Institute of Pharmaceutical Sciences, University of Graz, Graz, Austria

ARTICLE INFO

Article history:
Received 29 November 2010
Received in revised form 14 May 2011
Accepted 17 May 2011
Available online 2 June 2011

Keywords:
Tetraacetyl puerarin
Anti-oxidative
TNF-α
RAW264.7
Collagen-induced arthritis

ABSTRACT

Puerarin is a major active ingredient extracted from the root of *P. lobata*, a traditional Chinese herb, and possesses anti-oxidative and anti-inflammatory activities. However, the low oral bioavailability of puerarin limits its further application. Therefore, we synthesized tetraacetyl puerarin (4AC) through acetylation to improve its liposolubility and bioavailability. In the present investigations, we tested the anti-oxidative and TNF-α suppressive activity of 4AC in lipopolysaccharide (LPS)-induced RAW264.7 macrophages and bovine type II collagen-induced arthritic (CIA) rats. The results showed that 4AC retained the bioactivity of puerarin. And 4AC significantly increased the activity of SOD and reduced the level of MDA both in vitro and in vivo. It also improved the level of GSH-PX and the total antioxidant capacity in vivo. Furthermore, it dramatically decreased TNF-α level in the cultured supernatant of RAW264.7 cells treated with LPS and in the serum of CIA rats. These initial results indicated that 4AC had a potential therapeutic effect on CIA rats through an anti-oxidative and TNF-α suppressive activity. In addition, the molecular mechanism of anti-oxidation of 4AC was explored by testing the MAPKs/NF-κB signaling pathway. The results showed that 4AC significantly inhibited NF-κB expression and down-regulated the levels of p-ERK and p-JNK in LPS-activated RAW264.7 cells. These results indicated that 4AC had bioactive anti-oxidative effects and suggest the potential value of 4AC for the treatment of rheumatoid arthritis.

1. Introduction

Puerarin (*daidzein 8-C-glucoside*), the main isoflavone glucoside that is extracted from the root of *P. lobata* (also named *Radix Puerariae* or *Kudzu roots*), has been used for various medicinal purposes in traditional oriental medicine for thousands of years (Xiong et al., 2006). A few studies have revealed that puerarin possesses biological activities, such as anti-oxidative properties (Bebrevska et al., 2010; Hwang and Jeong, 2008), leading to increased superoxide dismutase activity and inhibition of the production of free radicals (Liu et al., 2000; Tan et al., 2008; Zhang et al., 2008). In addition, puerarin has a potential anti-inflammatory effect and may be a novel agent for the chemoprevention of atherosclerosis or inflammatory diseases (Hu et al., 2010). However, puerarin is restricted in application because of its poor oral bioavailability due to its high polarity and hydrophilicity, which reduces its affinity to enterocytes (Prasain et al., 2004). Accordingly, an increase in the liposolubility of puerarin might promote its absorption efficiency and prolong its elimination or metabolism times. 2″, 3″, 4″, 6″-tetraacetyl puerarin (4AC) has been synthesized by our group, and pharmacokinetic investigations show that the bioavailability of 4AC is clearly better than that of puerarin when tested in rats and Beagle dogs (Guo et al., 2008; Guo et al., 2009). However, it is not known whether 4AC retains the bioactivities of puerarin.

Oxidative stress and numerous inflammatory cytokines are clearly involved in the pathogenesis of various diseases, including rheumatoid arthritis. In addition, a pro-oxidant/anti-oxidant imbalance may be directly involved in the pathology of rheumatoid arthritis (Hitchon and El-Gabalawy, 2004; Shivani et al., 2003; Sweeney and Firestein, 2004; Yesim et al., 2007). Several lines of evidence suggest a pivotal role for oxygen radical generation and lipid peroxidation in the tissue damage in patients with rheumatoid arthritis (Ayhan et al., 2004). However, inflammatory mediators, such as tumor necrosis factor-

* Correspondence to: D. Yang, State Key Laboratory Incubation Base of Chinese Medicine and Molecular Pharmacology, Shenzhen 518057, China. Tel.: +86 755 26737139; fax: +86 755 26972852.
** Correspondence to: A. Lu, Institute of Basic Research in Clinical Medicine, China Academy of Chinese Medical Sciences, Beijing 100700, China. Tel.: +86 10 64067611; fax: +86 10 84032881.
E-mail addresses: yangdajian@yahoo.com (D. Yang), lap64067611@126.com (A. Lu).
[1] Both authors contributed equally to this work.

0014-2999/$ – see front matter © 2011 Elsevier B.V. All rights reserved.
doi:10.1016/j.ejphar.2011.05.061

alpha (TNF-α), are closely associated with the pathological process and play important roles in the early stage of rheumatoid arthritis (Feldmann et al., 1996). In the last decade, anti-TNF-α agents, such as infliximab, etanercept and adalimumab, have been launched and licensed as the first biological therapies for rheumatoid arthritis in clinical trials. Accordingly, TNF-α has become a promising target for drug screening and treatment strategies (Nam and Emery, 2010; Perdriger, 2009; Taylor and Feldmann, 2009). Many researchers have demonstrated that macrophages, which are the key inflammatory cells in joints with inflammation, are the major producers of TNF-α and multiple free radicals. Furthermore, macrophages express TNF-α through the MAPK/NF-κB signaling pathway in response to oxidative injury or an inflammatory stimulus (Parameswaran and Patial, 2010).

We recently reported that *anthocyanins*, one type of flavonoid that is extracted from cherries, down-regulates the levels of TNF-α in serum and improves the anti-oxidative status of arthritic rats (He et al., 2006). Therefore, similar bioactivities for 4AC were expected. In this study, the anti-oxidative properties and inhibitory effect of 4AC on TNF-α expression were explored in lipopolysaccharide (LPS)-activated RAW264.7 macrophages and CIA rats. NF-κB activation and the phosphorylation of ERK and JNK were tested in activated RAW264.7 cells to illuminate the initial mechanisms of the anti-oxidative and anti-inflammatory effects of 4AC.

2. Materials and methods

2.1. Chemicals and reagents

DMEM and fetal bovine serum (FBS) were purchased from Gibco (U.S.A.), and penicillin, streptomycin, trypsin–EDTA, and DMSO were purchased from Sigma-Aldrich (U.S.A.). Enhanced chemiluminescence (ECL) western blotting detection reagents and Hyperfilm ECL were obtained from Millipore Co. (U.S.A.). Anti-rabbit IgG (H + L) antibodies were purchased from Jackson (U.S.A.). Anti-mouse-p-p44/42 (Cat. 4370), anti-mouse-p44/42 (Cat. 4695), anti-p-SAPK/JNK (Cat. 4668) and SAPK/JNK (Cat. 9258) antibodies were purchased from C.S.T. (U.S.A.). Anti-mouse-NF-κB (p65), anti-mouse-β-actin and anti-mouse-GAPDH antibodies were purchased from Beijing Taihua Company (China). Soluble pure bovine type II collagen (Cat. 20022) and incomplete Freund's adjuvant (Cat. 7002) were purchased from Chondrex Inc. (U.S.A.). An anti-rat-TNF-α ELISA kit (Cat. BMS622) and an anti-mouse-TNF-α ELISA kit (Cat. BMS607) were purchased from Bender (Austria). MDA, total antioxidant capacity, SOD, GSH-PX assay kits and an ROS assay kit (DCFH-DA, Cat. S0033) were purchased from the Nanjing Jiancheng Bioengineering Institute (Nanjing, China). RAW264.7 cells (ATCC number: TIB-71) were obtained from the cell center of the Chinese Academy of Medical Sciences (CAMS).

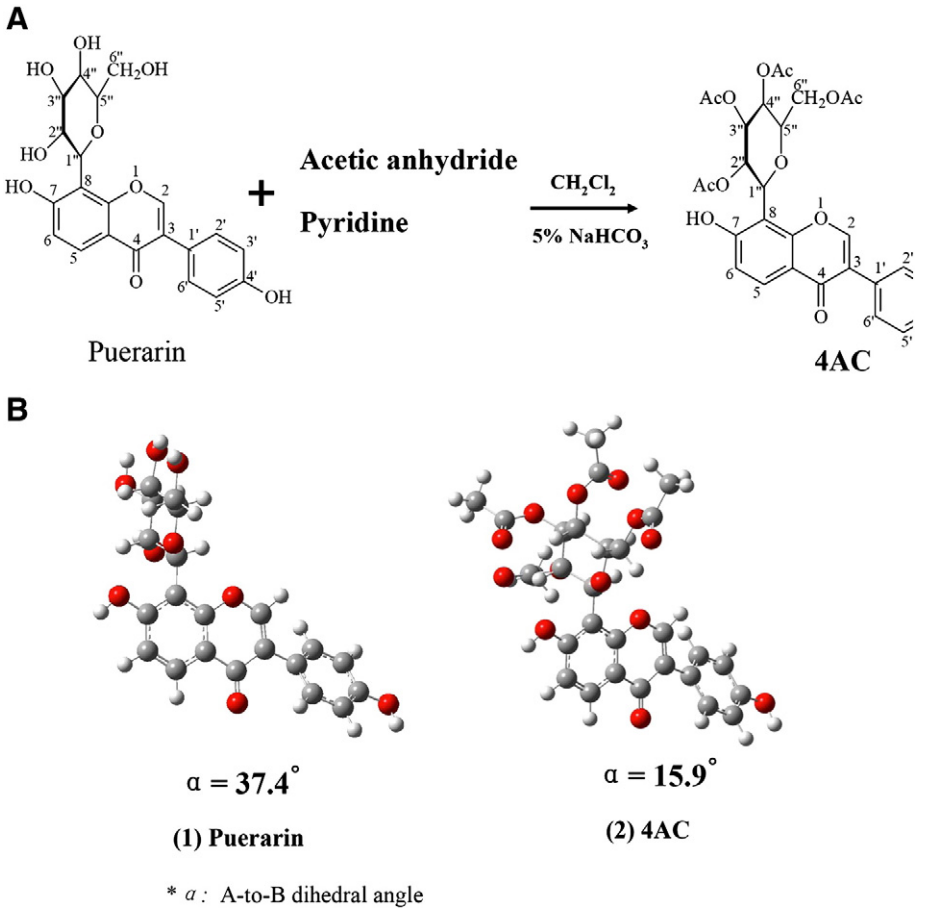

Fig. 1. Production of 2″, 3″, 4″, 6″-tetraacetyl puerarin (4AC), characterization, molecular geometries and physicochemical property. (A) The characterization of 4AC: mp 144–146 °C, UV–vis (MeOH/nm): λ = 205, 305 nm; IR (KBr) υ = 1620.6, 1754.7 cm^{-1}; ^1H NMR (400 MHz, $CDCl_3$) δ = 8.19 (1H, s, 2-H), 8.21 (1H, d, J = 9 Hz, 5-H), 7.01 (1H, d, J = 9 Hz, 6-H), 7.39 (2H, d, J = 9 Hz, 2′,6′-H), 6.88 (2H, d, J = 9 Hz, 3′,5′-H), 5.76 (1H, d, J = 9.6 Hz, 1″-H), 2.14 (3H, s, CH3CO), 2.09 (3H, s, CH3CO), 2.03 (3H, s, CH3CO), 2.01 (3H, s, CH3CO); HRMS calcd. For $C_{29}H_{28}O_{13}$ 585.1608, found 585.1616. (B) Molecular geometries (α shows A loop to B loop dihedral angle).

Table 1
The modeling and calculation results of puerarin and 4AC.

	Puerarin	4AC
ClogP	−0.03	1.64
ClogD	−0.56	1.11
μ	5.40	3.23

ClogP: calculated lipid/water partition coefficients. ClogD: calculated lipid/water distribution coefficients under pH 7.4, the physiological conditions. μ: dipole moment.

2.2. Synthesis and physicochemical properties of 2″, 3″, 4″, 6″-tetraacetyl puerarin (4AC)

Acetic anhydride (100 g, 0.98 mol) was added drop-wise over 30 min to a solution of puerarin (50 g, 0.12 mol) in pyridine (300 ml) while maintaining the temperature at 0–4 °C. After the addition of acetic anhydride, the reaction mixture was stirred for an additional 24 h at room temperature. The mixture was slowly added to ice water (500 g) and filtered to obtain 80 g of an off-white solid. The solid was dissolved in 200 ml CH_2Cl_2. Twenty milliliters of a $NaHCO_3$ aqueous solution (5%, w/w) was added to the solution and stirred for 1 h at room temperature. The organic layer was washed with brine, dried (Na_2SO_4) and evaporated to yield 70 g of the crude product. This crude product was purified by elution from silica gel with mixed solvents of ethyl acetate: petroleum ether = 1:4 (v/v), followed by crystallization from acetone to obtain 2″, 3″, 4″, 6″-tetraacetyl puerarin (4AC, 15.0 g, 21.3%). The chemical structure of 4AC was characterized using nuclear magnetic resonance (NMR), as shown in Fig. 1. The physicochemical properties and steric molecular geometries of puerarin and 4AC were evaluated using quantum chemical calculations.

2.3. Cell culture and treatments

RAW264.7 cells, which are murine macrophage-like cells, were cultured in DMEM supplemented with 10% heat-inactivated FBS,

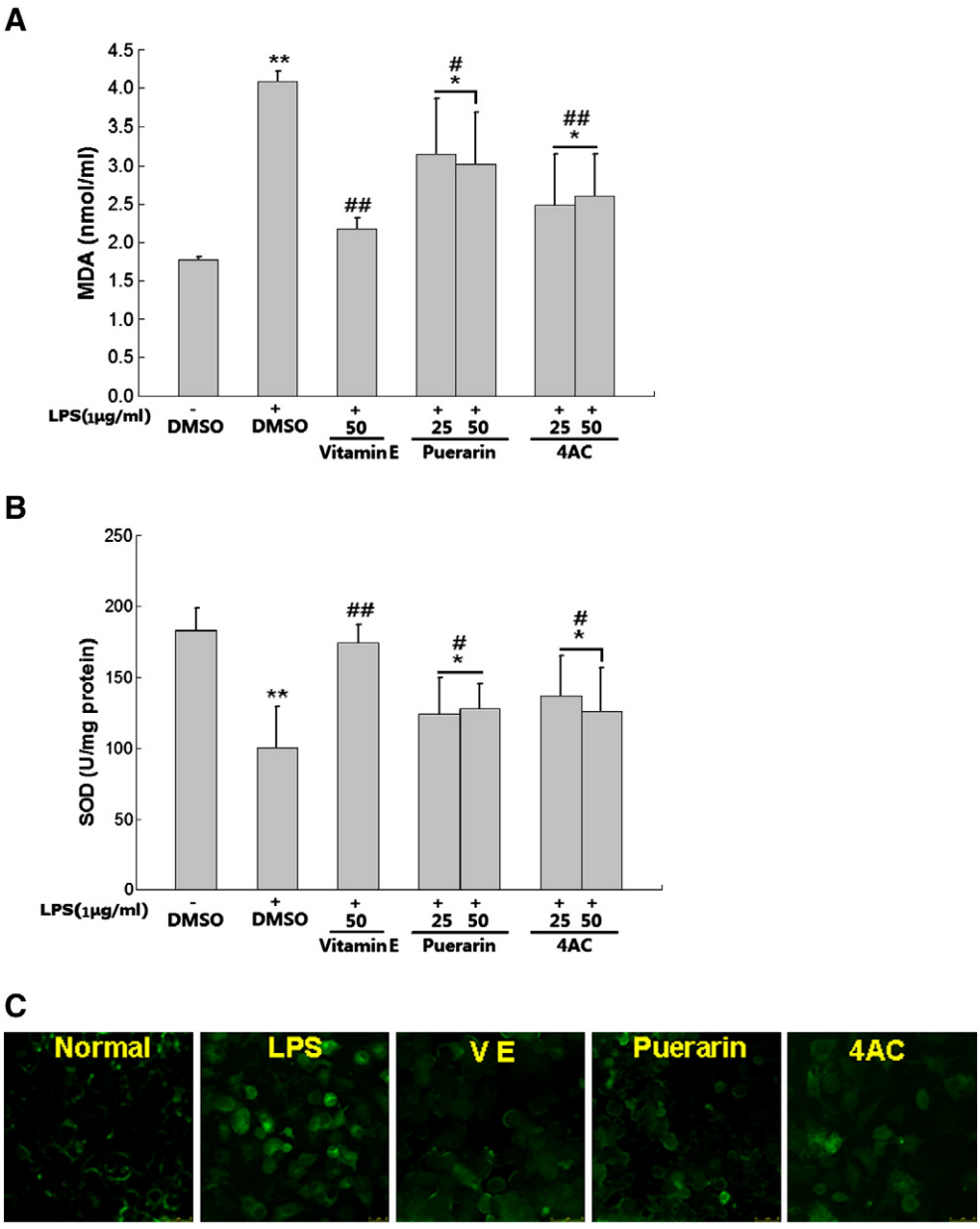

Fig. 2. Effects of puerarin and 4AC on the elimination of MDA and the increase in SOD activity. (A) MDA levels in homogenates of RAW264.7 cells; (B) SOD activity units in homogenates of RAW264.7 cells; (C) ROS scavenging activity and reducing capacity of 4AC and puerarin. DCHF fluorescence probe detected by confocal microscopy. Increased green fluorescence strength indicates higher ROS levels. * $P<0.05$; ** $P<0.01$ vs. normal control; # $P<0.05$; ## $P<0.01$ vs. LPS-induced model control (n = 8).

100 IU/ml of penicillin G and 100 μg/ml streptomycin under 5% CO_2 at 37 °C in a humidified atmosphere. Briefly, RAW264.7 cells were plated at a density of 2×10^5 cells/ml and serum-starved for 12 h. The cells were pretreated with puerarin or 4AC for 4 h prior to stimulation with LPS (1 μg/ml) for another 24 h. Puerarin and 4AC were freshly dissolved in DMSO on the day of the experiment and diluted with serum-free DMEM at appropriate concentrations. The final concentration of DMSO was adjusted to 0.1% (v/v). The control group received the same amount of DMSO.

2.4. Animals and experimental protocol

2.4.1. Induction of collagen induced arthritis

A total of 60 male Sprague–Dawley (SD) rats, 8–9 weeks old with a weight of 180 ± 15 g, were purchased from the Institute of Experimental Animals in the Chinese Academy of Medical Science (Rodent license no. SYXK 11-00-0039). The induction and assessment of collagen induced arthritis were performed as described previously (Cho et al., 2007; Hegen et al., 2008). Briefly, male SD rats were intradermally injected at the base of the tail with 200 μg bovine type II collagen in 0.05 M acetic acid emulsified with equal incomplete Freund's adjuvant. Seven days after the primary immunization, the rats received a booster with 100 μg collagen in the same manner as the primary immunization.

2.4.2. Administration of 4AC

4AC was administered orally in a volume of 1 ml/100 g body weight once a day beginning 12 days after the first immunization for 28 days. Sixty rats were divided randomly into 5 groups: 1) normal control group: non-arthritic rats with vehicle solution (DMEM mixed with saline); 2) CIA rats model group: CIA rats with vehicle control solution; 3) 4AC-high dose group: CIA rats with 90 mg/kg 4AC; 4) 4AC-low dose group: CIA rats with 45 mg/kg 4AC; and 5) dexamethasone group: CIA rats with 0.2 mg/kg dexamethasone. Rats were housed in a temperature/humidity/light controlled environment with free access to rodent feed and water. The light/dark cycle was 12 h:12 h, with the light phase from 06:00 to 18:00. The experimental procedures were reviewed and approved by the Animal Care and Use Committee in the China Academy of Chinese Medical Sciences before animal experiments were performed.

2.4.3. Arthritis assessment

Beginning 3 days after the boost, the degree of arthritis was examined every 2 days. The severity of arthritis was expressed as a mean arthritic index on a 0–4 scale according to the following criteria: 0 = no edema or swelling, 1 = swelling and erythema of the digit, 2 = slight edema and erythema that was limited to the foot and/or ankle, 3 = slight edema and erythema from the ankle to the tarsal bone, and 4 = severe edema and erythema from the ankle to the entire leg. Each posterior limb was graded, and the maximum possible score was 8 for each animal. A rat with a score of 1 or greater was regarded as arthritic (Larsson et al., 1990). The arthritis index was assessed during the experiment over 40 days. In addition, the histopathology of joint tissue was detected by H&E staining.

2.5. MTT assay for RAW264.7 cell viability

To measure cell viability, the MTT assay was performed as described previously. RAW264.7 cells were seeded in 96-well plates at 1×10^5 cells/ml and incubated in a 37 °C, 5% CO_2 incubator. After 24 h, the cells were pretreated with different concentrations of puerarin and 4AC (0, 5, 25, 50, 75, and 100 μM) for 4 h, followed by stimulation with LPS for 24 h. Subsequently, 5 mg/ml MTT was added to each well and incubated for an additional 4 h. The MTT medium in each well was carefully removed, and 100 μl DMSO was added to each well, followed by incubation at 37 °C for 10 min with gentle shaking. The absorbance at 570 nm was measured with a microplate reader (Labsystems, Multiskan Ascent Finland).

2.6. Antioxidant activity tests

2.6.1. Determination of MDA and SOD activity in RAW264.7 cells

RAW264.7 cells were seeded in a 24-well plate. The treatment procedure of LPS and test compounds was the same as described previously. Briefly, after treatment with LPS, puerarin and 4AC, the cells were washed rapidly with PBS, harvested and immediately homogenized on ice in 9 volumes of saline. The homogenates were centrifuged at 4000 rpm at 4 °C for 10 min. The content in the supernatants was measured using an MDA and SOD assay kit. The absorbance at 450 nm was measured with a microplate reader.

2.6.2. Estimation of ROS ability using a DCFH-DA assay in RAW264.7 cells

RAW 264.7 cells were seeded at 1×10^5 cells/ml in special culture dishes for confocal microscopy. After treatment with LPS and test compounds (i.e., the same procedure as mentioned above), 10 μl of DCFH-DA was added to the culture media for 20 min. Following the instructions of the commercially assay kits, RAW264.7 cells were washed abundantly and examined under a confocal microscope.

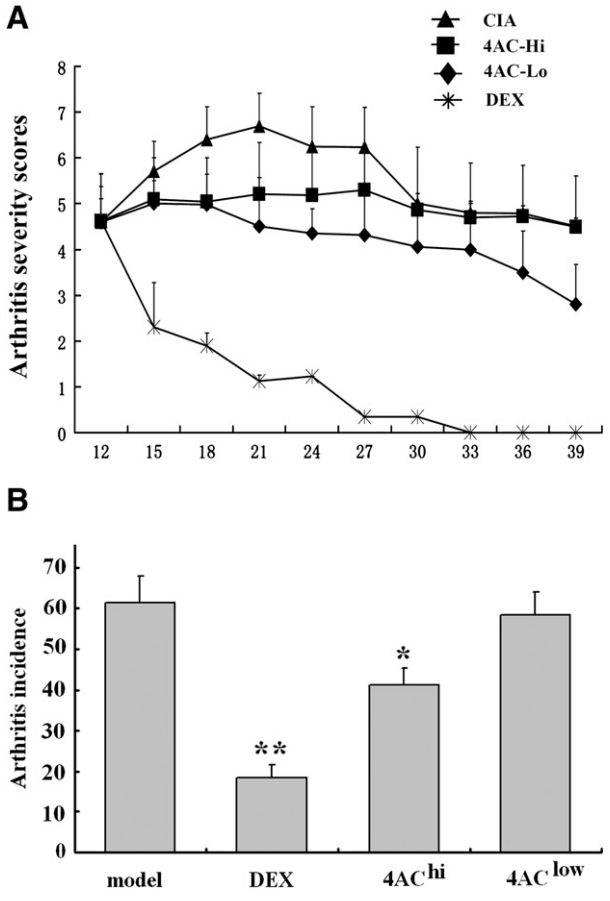

Fig. 3. The therapeutic effect of 4AC in CIA rats. (A) The arthritic scores on different days after immunization with bovine type II collagen. Arthritic scores tended to decrease in both low-dose and high-dose 4AC treatment groups compared to the CIA model group. (B) Arthritic incidence of CIA after treatment (28 days). The arthritic incidence in the high-dose 4AC group was lower than that in the CIA model group (61.5% vs. 40.3%, $P<0.05$).

2.6.3. Detection of MDA, SOD, GSH-PX levels and total anti-oxidation competence in hepatic tissue

After the rats were sacrificed, the hepatic tissue (n = 5) was collected, rinsed, weighed (2 g) and put into tubes with 9 ml saline. The tubes were homogenized for 10 min. After centrifugation at 3000 rpm for 10 min at 4 °C, the supernatants were collected immediately for the assays of MDA, SOD, GSH-PX and total antioxidant capacity. All of these measurements were determined using commercially available assay kits and were performed according to the manufacturer's recommendations. The absorbance at 450 nm was measured using a microplate reader.

2.7. ELISA for the detection of TNF-α levels in cultured supernatants and rat sera

The concentration of TNF-α in the cultured supernatants of RAW264.7 cells and the blood serum of rats were analyzed using commercially available ELISA kits according to the manufacturer's protocol. Briefly, RAW264.7 cells were seeded in 24-well plates at 2×10^5 cells/ml with 500 μl complete medium and allowed to attach for 24 h. Cells were incubated with puerarin and 4AC (25 or 50 μM) followed by the addition of LPS. After incubation for 8 h, the supernatants from the cells were collected. For the in vivo studies, blood serum was harvested after the rats were sacrificed. All of the samples were diluted at 1:10. The absorbance was read at 450 nm using a microplate reader. Samples and standards were run 3 times.

2.8. Western blotting to detect NF-κB, p-ERK, ERK, p-JNK, and JNK expression in RAW264.7 cells

RAW264.7 cells (2×10^5 cells/ml) were cultured in 6-well plates for 24 h. Cells were treated with 25 or 50 μM 4AC or puerarin for 4 h before the addition of 1 μg/ml LPS. The treatment procedure was the same as above. Whole-cell lysates were prepared using ice-cold cell lysis buffer. Protein concentration was determined using a BCA protein assay kit. Samples of cell lysates were separated by 10% SDS-PAGE and transferred onto polyvinylidene difluoride membranes. The membranes were immunoblotted with primary antibodies that recognize MAPKs (1:4000 ERK, 1:2000 JNK, 1:2000 p-ERK, 1:2000 p-JNK, 1:5000 β-actin, 1:5000 GADPH and 1:200 p65). Peroxidase-conjugated secondary antibodies and an ECL detection system were used according to routine methods. The intensities of the protein bands were analyzed using Gel-Pro 3.2 software. β-actin or GADPH protein was used as the internal control to normalize for protein loading.

2.9. Statistical analysis

Data are expressed as the mean ± S.D. Differences between the mean values of normally distributed data were assessed using a one-way ANOVA (Dunnett's *t* test) and the Student-Newman–Keuls test with SPSS 11.0 software. Analyses were performed using Excel and Paint software of Windows. Values of $P<0.05$ were regarded as statistically significant.

3. Results

3.1. Structure and physicochemical property of 4AC

The chemical structures and stereo-conformations of puerarin and 4AC are shown in Fig. 1(A–B). To obtain a comparison of the physicochemical properties of the two compounds, the lipid/water partition coefficients (ClogP), pH-dependent distribution coefficients (ClogD), and dipole moment (μ) were theoretically calculated using quantum chemistry methods for both puerarin and 4AC. Based on the

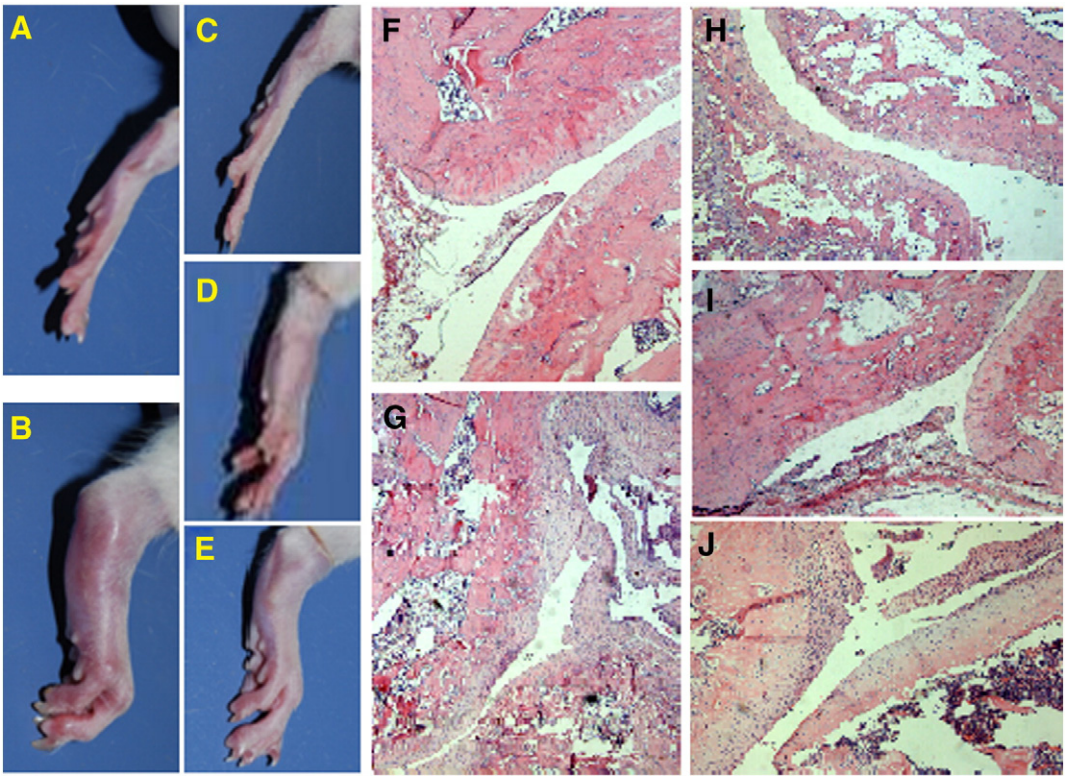

Fig. 4. Morphological and histopathological features of representative ankle joints. (A) Normal control rat; (B) swollen joint of a CIA rat; (C) DEX-treated rat; (D) high-dose 4AC-treated rat; (E) low-dose 4AC-treated rat; (F) normal histological features of joint tissue; (G) CIA rats showed a marked infiltration of inflammatory cells and a narrow joint space with synovial hyperplasia; (H) CIA rats treated with dexamethasone; (I) CIA rats treated with high-dose 4AC; and (J) CIA rats treated with low-dose 4AC. Dexamethasone or 4AC showed less inflammatory cell infiltration, well-preserved joint spaces and minimal synovial hyperplasia. H–J from H&E stain (×100).

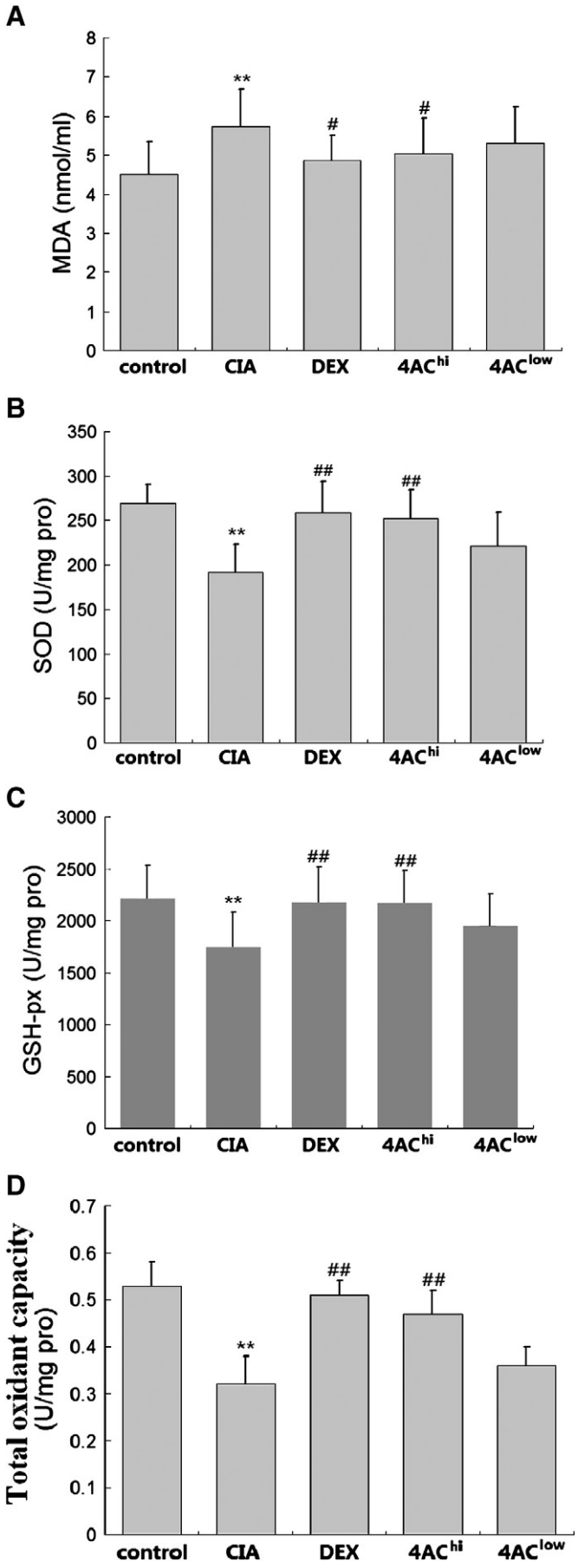

higher ClogP and ClogD and lower μ of 4AC than puerarin (Table 1), 4AC clearly had higher liposolubility and lower polarity than puerarin.

3.2. Effect of puerarin and 4AC on RAW264.7 cell viability

Puerarin and 4AC (1–75 μM) did not display any cellular toxicity in RAW264.7 cells over 24 h, as determined by the MTT assay (data not shown).

3.3. In vitro anti-oxidation activities of puerarin and 4AC

In the present investigation, MDA levels were strongly increased in LPS-activated RAW264.7 cells. Both puerarin and 4AC significantly inhibited the production of MDA. As shown in Fig. 2A, 4AC and puerarin dramatically suppressed LPS-mediated oxidation. Among the antioxidant systems, SOD is a major scavenger of ROS. The level of SOD activity increased remarkably after treatment with 4AC and puerarin (Fig. 2B). SOD and MDA inhibitory activities were not positively associated with 4AC or puerarin concentrations. Under the same experimental conditions, 4AC and puerarin showed weaker activity than Vitamin E, a positive antioxidant.

The effects of 4AC and puerarin on ROS scavenging activity and reducing power were further examined using DCHF, which is a fluorescent probe. In Fig. 2C, the fluorescence strength was reduced in 4AC- and puerarin-treated cells compared to LPS-activated cells.

3.4. Effect of 4AC on CIA rats

All animals tolerated the experimental procedures well, and no deaths occurred during the 40-day study. The onset and distribution of arthritis were similar to the patterns we have described previously (Zhou et al., 2006). Fig. 3A summarizes arthritic scores beginning on day 14 after the immunization. The arthritic scores decreased in rats that were treated with 4AC at the high dose, especially during the early stage from day 14 to day 20. The total arthritic incidence of CIA in the group with the higher dose of 4AC was lower than that in the CIA group (Fig. 3B). However, there was no significant difference in arthritic incidence between the rats in the low-dose 4AC and the CIA groups, which indicated that the CIA activity of 4AC was not positively associated with concentration.

We analyzed the histopathology of the ankle joints to determine whether 4AC prevented articular destruction. Fig. 4B shows that there was significant swelling in the hind paws of CIA rats compared to normal rats (Fig. 4A). There was no particular swelling in the dexamethasone group (Fig. 4C) or the high-dose 4AC group (Fig. 4D). As shown in Fig. 4G, the infiltration of inflammatory cells and synovial hyperplasia in CIA rats was clear. However dexamethasone and 4AC treatment can alleviate those changes of pathology (Fig. 4H–J), which showed a potential therapeutic effect of 4AC.

3.5. Anti-oxidative capacity of 4AC in vivo

The change in SOD, MDA, GSH-PX levels and total antioxidant capacity in hepatic tissue after treatment with 4AC is shown in Fig. 5. Compared to normal rats, the levels of SOD, GSH-PX and total antioxidant capacity were significantly reduced in CIA rats, but the MDA level was greatly increased. Dexamethasone and the high dose of 4AC treatment enhanced the levels of SOD, GSH-PX and the total antioxidant capacity, but reduced the level of MDA significantly.

Fig. 5. Effect of 4AC on SOD, MDA, GSH-PX and T-AOC levels in hepatic tissue. (A) MDA level, (B) SOD level, (C) GSH-PX level, (D) total antioxidant capacity. Rats were treated with either PBS (0.2 mg/kg/day), dexamethasone (0.2 mg/kg/day), high-dose 4AC (90 mg/kg/day) or low-dose 4AC (45 mg/kg/day). The results are shown as the mean ± S.D. ** $P<0.01$ vs. normal control group; $^{\#}$ $P<0.05$; $^{\#\#}$ $P<0.01$ vs. CIA control group (n = 8).

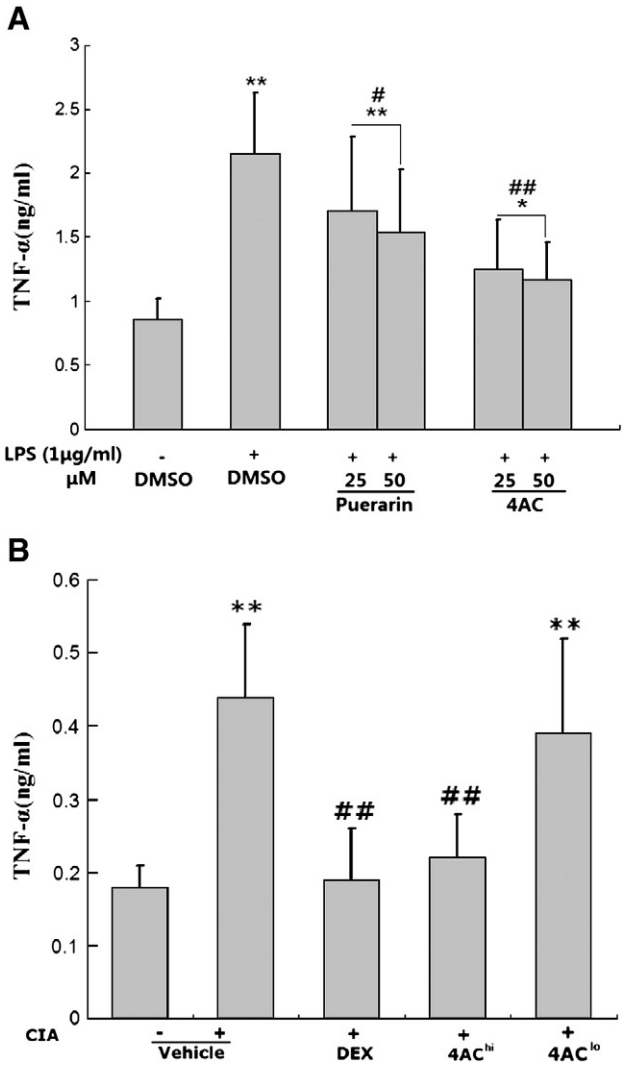

Fig. 6. The effect of 4AC on TNF-α level in the supernatant of cultured RAW264.7 cells and in the serum of rats. (A) Levels of TNF-α in the cultured supernatant of RAW264.7 cells; (B) levels of TNF-α in the serum of CIA rats. Data are the means ± S.D. ** $P<0.01$ vs. normal control; # $P<0.05$, ## $P<0.01$ vs. model control (n = 8).

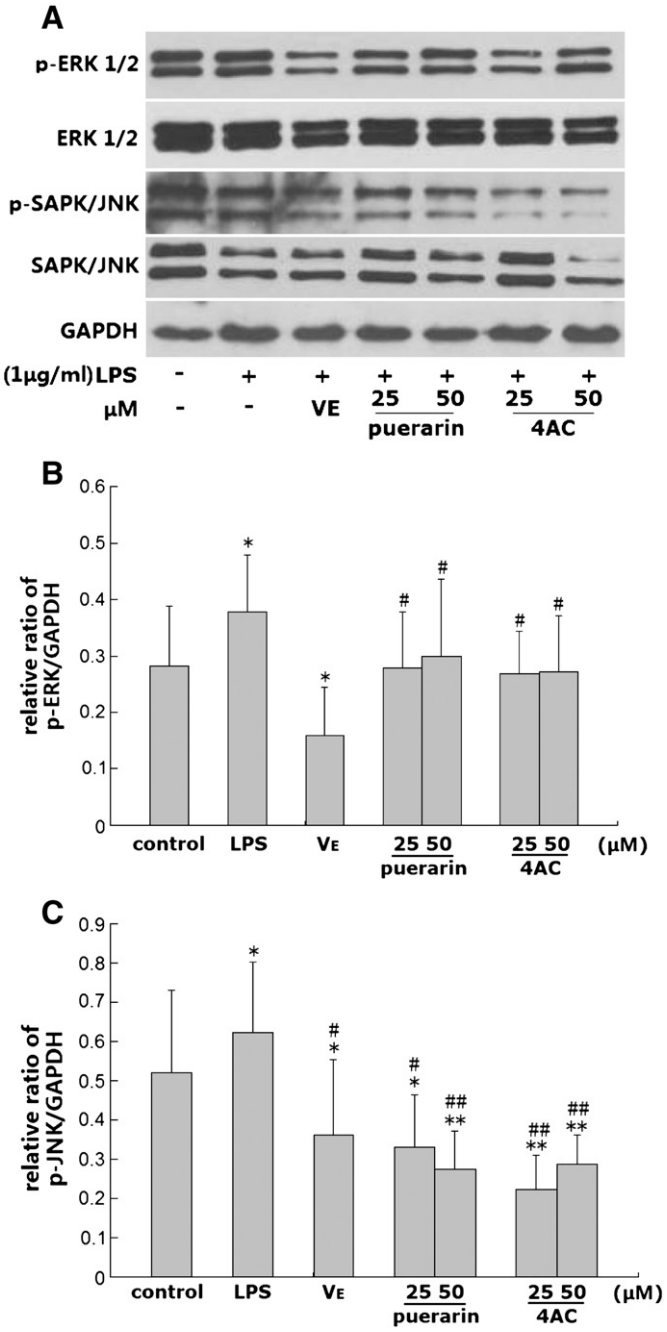

Fig. 7. Effect of 4AC and puerarin on LPS-induced phosphorylation of MAPKs in RAW264.7 cells. RAW264.7 cells were treated with 25 or 50 μM 4AC or puerarin for 4 h before the addition of 1 μg/ml LPS for 1 h. Cell extracts were subjected to western blot analysis with phosphor-specific antibodies. The total MAPK and GAPDH levels were used as internal controls. (A) Western blot of the MAPK isoforms; (B) relative ratio of p-ERK, means ± S.D. of three independent experiments; (C) relative ratio of p-JNK. * $P<0.05$; ** $P<0.01$ vs. normal control; # $P<0.05$; ## $P<0.01$ vs. LPS-induced model control.

3.6. Effect on the levels of TNF-α by 4AC in vitro and in vivo

To investigate the anti-inflammatory effects of 4AC and puerarin, we quantified TNF-α production in the supernatant of cultured RAW264.7 cells. As shown in Fig. 6A, TNF-α level markedly increased after exposure to LPS alone. Treatment with 4AC and puerarin inhibited LPS-induced TNF-α production.

The in vivo TNF-α inhibitory activity of 4AC was tested using an ELISA method. As shown in Fig. 6B, the levels of TNF-α in sera were significantly increased in CIA rats. In addition, the levels of TNF-α decreased in the dexamethasone and high-dose 4AC groups. However, there was no significant difference in the levels of TNF-α between the low dose 4AC-treated rats and the CIA rats, which suggested that 4AC possessed the dose dependent in pharmacodynamics.

3.7. Puerarin and 4AC suppressed the phosphorylation of ERK and JNK in LPS-stimulated RAW264.7 cells

MAPK signaling pathways were investigated to determine the expression of pro-inflammatory mediators by activated macrophages during oxidative damage and the inflammatory response. To determine whether MAPK signaling pathways were involved in the anti-oxidation and anti-inflammatory effects of 4AC and puerarin, the phosphorylation of two MAPK signaling molecules, ERK and JNK, was examined by western blot analysis. Fig. 7A–C shows that the levels of p-ERK and p-JNK were dramatically decreased in 4AC- and puerarin-treated cells compared to the cells treated with LPS only. However, the total levels of ERK and JNK did not differ significantly between these groups. These data indicated that signal transduction by MAPK molecules might be effectively influenced by 4AC and puerarin.

3.8. Puerarin and 4AC prevented NF-κB activation in LPS-stimulated RAW264.7 cells

NF-κB is an important transcription factor that is involved in TNF-α production in LPS-activated macrophages. We investigated whether 4AC and puerarin had an inhibitory effect on NF-κB expression. As shown in Fig. 8A, the NF-κB (p65) levels were increased significantly in LPS-stimulated RAW264.7 cells. However, the levels of NF-κB were markedly attenuated in Vitamin E-, 4AC-, and puerarin-treated cells. More remarkably, 4AC, especially at a high dose, produced a dramatic inhibitory effect on NF-κB levels compared to puerarin (Fig. 8B). This result suggested that 4AC had a potential role in the suppression of the NF-κB signaling pathway in inflammation-mediated TNF-α production.

4. Discussion

Puerarin is the major isoflavonoid derived from the Chinese medical herb *Radix pueraria lobatae* (*called Gegen in Chinese*). Puerarin has good antioxidant activity, which occurs through multiple mechanisms, such as the scavenging of free radicals, increasing SOD activity and decreasing MDA (Xiong et al., 2006). Researchers have also shown that puerarin has an effect in treating coronary heart disease (Yan et al., 2006). However, bad oral bioavailability is the shortcoming for its clinical application. The puerarin derivative 4AC, which is synthesized through acetylation, greatly improves liposolubility. A pharmacokinetic investigation has shown that puerarin and 4AC are fitted to a two-compartment model in rats and beagles, which suggests that 4AC improves bioavailability (Guo et al., 2008; Guo et al., 2009). We also calculated the lipid/water partition coefficients (C-logP and C-logD) and the dipole moment (μ), and the results were consistent with our experimental data from pharmacokinetic experiments. In fact, it was difficult to define the efficiency of the digestive absorption of isoflavonoids. Researchers have suggested that an enhancement of water solubility may strongly increase the bioavailability and bioactivity of puerarin (Chung et al., 2008). These paradoxical experimental data indicate that the bioactivity of natural compounds is affected by multiple pathways.

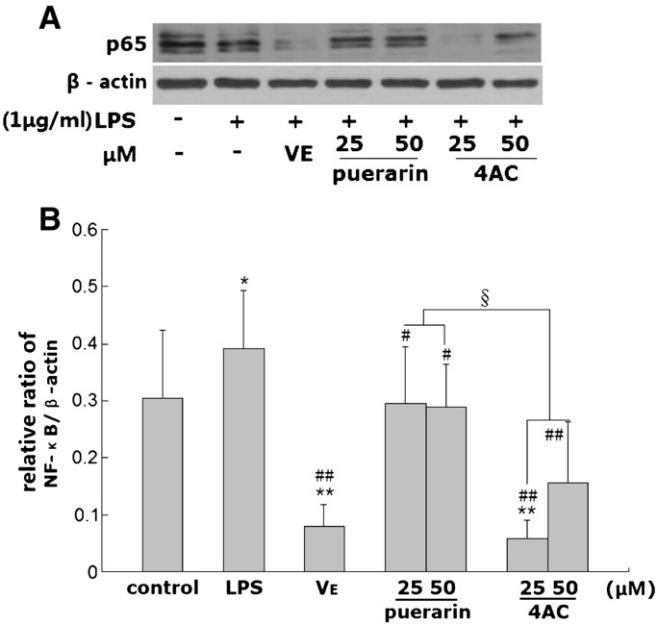

Fig. 8. 4AC suppressed LPS-induced NK-κB expression in RAW264.7 cells. RAW264.7 cells were treated with 25 or 50 μM 4AC or puerarin for 4 h before the addition of 1 μg/ml LPS for 1 h. The cells were harvested and extracted for the detection of the total forms of NF-κB p-65 subunit using western blotting. (A) A representative western blot; (B) means ± S.D. of three independent experiments. * $P<0.05$; ** $P<0.01$ vs. normal control; # $P<0.05$; ## $P<0.01$ vs. LPS-induced model control.

Oxidative damage by oxygen free radicals to essential cell components is a serious mechanism in the pathogenesis of many diseases, including tumors, cardiovascular diseases, diabetes, and rheumatoid arthritis. Rheumatoid arthritis is a systemic autoimmune disease that is characterized by chronic synovitis. Although the etiology of rheumatoid arthritis remains unclear, evidence has indicated that free radicals are involved in the occurrence and development of this disease (Hitchon and El-Gabalawy, 2004; Vasanthi et al., 2009). In the inflammatory lesions in the synovium and during the bone destruction process, free radicals are directly or indirectly involved in damage to the synovial membrane and bone. Increased lipid peroxidation and decreased enzymatic and non-enzymatic antioxidants are found in rheumatoid arthritic patients, and this evidence suggests that oxidant stress plays a very important role in the pathogenesis of this disease (Kamanli et al., 2004). MDA levels in patients with rheumatoid arthritis are significantly higher than those in controls, but the activities of GSH-PX and SOD are lower. These results indicate that there is an increase in oxidative stress and a low antioxidant status in patients with rheumatoid arthritis (Karatas et al., 2003). In addition, studies have also evaluated the importance of antioxidant therapy in the management of rheumatoid arthritis and have suggested the necessity of a therapeutic co-administration of antioxidants with conventional drugs to patients with this disease (Jaswal et al., 2003). One study has shown that gavage with oral vitamin E prevents joint destruction in a mouse model of rheumatoid arthritis (De Bandt et al., 2002). In this study, we showed that 4AC significantly increased the activity of SOD and reduced the levels of MDA both in vitro and in vivo. Based on the results of the DCFH assay and the total antioxidant capacity examination, we determined that 4AC retained strong anti-oxidative activity. Our initial results indicated that one mechanism of 4AC in CIA rats may be to suppress the pathological state of arthritis by anti-oxidation.

In recent years, biological therapies have become a hot topic for the treatment of various diseases. Inhibitors of TNF-α are most widely used in inflammatory diseases, including rheumatoid arthritis, atherosclerosis, psoriasis, diabetes and Crohn's disease (Parameswaran and Patial, 2010). TNF-α is not only the 'master-regulator' of inflammation in synovium but also contributes significantly to articular destruction in human rheumatoid arthritis (Furst, 2010). The overproduction of TNF-α stimulates cartilage matrix degradation by inhibiting the production of proteoglycans and type II collagen and up-regulating the production of matrix-degrading enzymes, such as matrix metalloproteinases (MMPs) (Goldring, 2000). The blockade and inhibition of TNF-α suppress the pathological processes of rheumatoid arthritis (Takeuchi et al., 2007). Our results showed that TNF-α levels were decreased significantly in the cultured supernatants of 4AC- and puerarin-treated RAW264.7 cells. These same results were observed in the serum of CIA rats that were treated with a high dose of 4AC. These results suggest that 4AC has a potential anti-inflammatory function.

To investigate the protective mechanism of anti-oxidation and anti-inflammation of 4AC, we explored the expression of NF-κB, which is the main regulator of most pro-inflammatory genes. In LPS-activated RAW264.7 cells, the levels of NF-κB were up-regulated remarkably. However, 4AC produced a novel inhibitory effect, which indicated that NF-κB pathways might be involved in the suppressive effects of 4AC on the release of TNF-α.

MAPKs are a family of serine/threonine protein kinases that are responsible for most of the cellular responses to cytokines and are crucial for the regulation of the production of inflammatory mediators (Cao et al., 2008). Therefore, these pathways may involve the molecular mechanisms of the anti-oxidative and TNF-α inhibitory effects of 4AC. In our experiments, the phosphorylation levels of ERK and JNK were rapidly up-regulated in RAW264.7 cells induced by LPS, but down-regulated significantly by 4AC and

puerarin. These results suggest that 4AC affects MAPK signaling cascade. Our results are in agreement with most studies that many natural products inhibit the expression of pro-inflammatory genes by modulating the phosphorylation of members of the MAPK pathway (Chen et al., 2008; Cheng et al., 2008).

In summary, the present study shows that 4AC, the newly synthesized puerarin derivative, is a fully active isoflavone that has good antioxidant reactivity and TNF-α-suppressive effects. Its therapeutic effect in CIA rats may have been partially associated with its ability to inhibit the production of inflammatory mediators (e.g., TNF-α) via the inhibition of the activation of the MAPK/NF-κB pathway.

Acknowledgments

This study is supported in part by the projects from Shenzhen–Hong Kong Innovation Circle Funding Program, Ministry of Sciences and Technology (No. 2009ZX09502-019 and 2009ZX09103-150) and National Science Foundation of China (No. 30825047 and 30902000). Many thanks to Dr. Ruimin Han, the staff of the Department of Chemistry of Renmin University of China, for providing the theoretical calculation of the physicochemical properties of puerarin and 4AC.

References

Ayhan, K., Mustafa, N., Nurettin, A., Cengiz, H., 2004. Plasma lipid peroxidation and antioxidant levels in patients with rheumatoid arthritis. Cell Biochem. Funct. 22, 53–57.

Bebrevska, L., Foubert, K., Hermans, N., Chatterjee, S., Van Marck, E., De Meyer, G., Vlietinck, A., Pieters, L., Apers, S., 2010. In vivo antioxidative activity of a quantified puerarin lobata root extract. J. Ethnopharmacol. 127, 112–117.

Cao, W., Bao, C., Padalko, E., Lowenstein, C.J., 2008. Acetylation of mitogen-activated protein kinase phosphatase-1 inhibits Toll-like receptor signaling. J. Exp. Med. 205, 1491–1503.

Chen, C.C., Tsai, P.C., Wei, B.L., Chiou, W.F., 2008. 8-Prenylkaempferol suppresses inducible nitric oxide synthase expression through interfering with JNK-mediated AP-1 pathway in murine macrophages. Eur. J. Pharmacol. 590, 430–436.

Cheng, Y.W., Chang, C.Y., Lin, K.L., Hu, C.M., Lin, C.H., Kang, J.J., 2008. Shikonin derivatives inhibited LPS-induced iNOS in RAW 264.7 cells via downregulation of MAPK/NF-kB signaling. J. Ethnopharmacol. 120, 264–271.

Cho, Y.G., Cho, M.L., Min, S.Y., Kim, H.Y., 2007. Type II collagen autoimmunity in a mouse model of human rheumatoid arthritis. Autoimmun. Rev. 7, 65–70.

Chung, M.J., Sung, N.J., Park, C.S., Kweon, D.K., Mantovani, A., Moon, T.W., Lee, S.J., Park, K.H., 2008. Antioxidative and hypocholesterolemic activities of water-soluble puerarin glycosides in HepG2 cells and in C57BL/6J mice. Eur. J. Phamacol. 578, 159–170.

De Bandt, M., Grossin, M., Driss, F., Pincemail, J., Babin-Chevaye, C., Pasquier, C., 2002. Vitamin E uncouples joint destruction and clinical inflammation in a transgenic mouse model of rheumatoid arthritis. Arthritis Rheum. 46, 522–532.

Feldmann, M., Brennan, F.M., Maini, R.N., 1996. Role of cytokines in rheumatoid arthritis. Aunu. Rev. Innunol. 14, 397–440.

Furst, D.E., 2010. Development of TNF inhibitor therapies for the treatment of rheumatoid arthritis. Clin. Exp. Rheumatol. 28, S5–S12.

Goldring, M.B., 2000. The role of the chondrocyte in osteoarthritis. Arthritis Rheum. 43, 1916.

Guo, D., Yang, D., Chen, S., 2008. Pharmacokinetic investigation of puerarin and derivatives in rats. Journal of Shanxi College of Traditional Chinese Medicine. 31, 52–55 (in Chinese).

Guo, D., Chen, S., Yang, D., 2009. Pharmacokinetic investigation of suspension and nanoparticles of puerarin derivative 4AC in Beagle dogs. Li Shi Zhen Medicine and Materia Medica research. 20, 197–198 (in Chinese).

He, Y.H., Zhou, J., Wang, Y.S., Xiao, C., Tong, Y., Tang, J.C., Chan, A.S., Lu, A.P., 2006. Anti-inflammatory and anti-oxidative effects of cherries on Treund's adjuvant-induced arthritis in rats. Scand. J. Rheumatol. 35, 356–358.

Hegen, M., Keith Jr., J.C., Collins, M., Nickerson-Nutter, C.L., 2008. Utility of animal models for identification of potential therapeutics for rheumatoid arthritis. Ann. Rheum. Dis. 67, 1505–1515.

Hitchon, C.A., El-Gabalawy, H.S., 2004. Oxidation in rheumatoid arthritis. Arthritis Res. Ther. 6, 265–278.

Hu, W., Zhang, Q., Yang, X., Wang, Y., Sun, L., 2010. Puerarin inhibits adhesion molecule expression in TNF-alpha-stimulated human endothelial cells via modulation of the nuclear factor kappaB pathway. Pharmacol. 85, 27–35.

Hwang, Y.P., Jeong, H.G., 2008. Mechanism of phytoestrogen puerarin-mediated cytoprotection following oxidative injury: estrogen receptor-dependent up-regulation of PI 3K/Akt and HO-1. Toxicol. Appl. Pharmacol. 233, 371–381.

Jaswal, S., Mehta, H.C., Sood, A.K., Kaur, J., 2003. Antioxidant status in rheumatoid arthritis and role of antioxidant therapy. Clin. Chim. Acta 338, 123–129.

Kamanli, A., Naziroğlu, M., Aydilek, N., Hacievliyagil, C., 2004. Plasma lipid peroxidation and antioxidant levels in patients with rheumatoid arthritis. Cell Biochem. Funct. 22, 53–57.

Karatas, F., Ozates, I., Canatan, H., Halifeoglu, I., Karatepe, M., Colakt, R., 2003. Antioxidant status and lipid peroxidation in patients with rheumatoid arthritis. Indian J. Med. Res. 118, 178–181.

Larsson, P., Kleinau, S., Holmdahl, R., Klareskog, L., 1990. Homologous type II collagen-induced arthritis in rats. Characterization of the disease and demonstration of clinically distinct forms of arthritis in two strains of rats after immunization with the same collagen preparation. Arthritis Rheum. 33, 693–701.

Liu, Q., Lu, Z., Wang, L., 2000. Restrictive effect of puerarin on myocardial infarct area in dogs and its possible mechanism. J. Tongji Med. Univ. 20, 43–45 (in Chinese).

Nam, J., Emery, P., 2010. Aspects of TNF inhibitor therapy in rheumatoid arthritis. Mod. Rheumatol. 20, 325–330.

Parameswaran, N., Patial, S., 2010. Tumor necrosis factor-α signaling in macrophages. Crit. Rev. Eukaryot. Gene Expr. 20, 87–103.

Perdriger, A., 2009. Infliximab in the treatment of rheumatoid arthritis. Biologics. 3, 183–191.

Prasain, J.K., Jones, K., Brissie, Moore, R., Wyss, J.M., Barnes, S., 2004. Identification of puerarin and its metabolites in rats by liquid chromatography–tandem mass spectrometry. J. Agric. Food Chem. 52, 3708–3712.

Shivani, J., Harish, C.M., Arun, K.S., Jasinder, K., 2003. Antioxidant status in rheumatoid arthritis and role of antioxidant therapy. Clinica Chimica Acta. 338, 123–129.

Sweeney, S.E., Firestein, G.S., 2004. Rheumatoid arthritis: regulation of synovial inflammation. Int. J. Biochem. Cell Biol. 36, 372–378.

Takeuchi, T., Nakanishi, T., Tabushi, Y., Hata, A., Shoda, T., Kotani, T., Shimizu, A., Takubo, T., Makino, S., Hanafusa, T., 2007. Serum protein profile of rheumatoid arthritis treated with anti-TNF therapy (infliximab). J. Chromatogr. B Analyt. Technol. Biomed. Life Sci. 855, 66–70.

Tan, Y., Liu, M., Wu, B., 2008. Puerarin for acute ischemic stroke. Stroke 39, 2188.

Taylor, P.C., Feldmann, M., 2009. Anti-TNF biologic agents: still the therapy of choice for rheumatoid arthritis. Nat. Rev. Rheumatol. 5, 578–582.

Vasanthi, P., Nalini, G., Rajasekhar, G., 2009. Status of oxidative stress in rheumatoid arthritis. Int. J. Rheum. Dis. 12, 29–33.

Xiong, F.L., Sun, X.H., Gan, L., Yang, X.L., Xu, H.B., 2006. Puerarin protects rat pancreatic islets from damage by hydrogen peroxide. Eur. J. Pharmacol. S29, 1–7.

Yan, L.P., Chan, S.W., Chan, A.S.C., Chen, S.L., Ma, X.J., Xu, H.X., 2006. Puerarin decreased serum total cholesterol and enhances thoracic aorta endothelial nitric oxide synthase expression in diet-induced hypercholesterolemic rats. Life Sci. 79, 324–330.

Yesim, O., Sevgi, Y.A., Aylin, S., Erinc, K., Vesile, S., Bolkan, S., 2007. Oxidative status in rheumatoid arthritis. Clin. Rheumatol. 26, 64–68.

Zhang, S.Y., Chen, G., Wei, P.F., Huang, X.S., Dai, Y., Shen, Y.J., Chen, S.L., Sun-chi, C.A., Xu, H.K., 2008. The effect of puerarin on serum nitric oxide concentration and myocardial eNOS expression in rats with myocardial infarction. J. Asian Nat. Prod. Res. 10, 373–381.

Zhou, J., Xiao, C., Zhao, L., Jia, H., Zhao, N., Lu, C., Tang, J.C., Chan, A.S., Lu, A.P., 2006. The effect of triptolide on $CD4^+$ and $CD8^+$ cells in Peyer's patch of SD rats with collagen induced arthritis. Int. Immunopharmacol. 6, 198–203.